Bimodal determination of immunoglobulin E by fluorometry and ICP-MS by using platinum nanoclusters as immunoassay labels

Ana Lores-Padín[1], María Cruz-Alonso[1], Héctor González-Iglesias[2,3*], Beatriz Fernández[1,2*] and Rosario Pereiro[1,2]

[1]Department of Physical and Analytical Chemistry, University of Oviedo, Julian Clavería 8, 33006 Oviedo, Spain.

[2]Instituto Universitario Fernández-Vega (Fundación de Investigación Oftalmológica, Universidad de Oviedo), Avda. Dres. Fernández-Vega, 34, 33012 Oviedo, Spain.

[3]Instituto Oftalmológico Fernández-Vega, Avda. Dres. Fernández-Vega, 34, 33012 Oviedo, Spain.

*Corresponding authors email address:

fernandezbeatriz@uniovi.es (phone number +34.985.10.3524)

h.gonzalez@fio.as (phone number +34.985.24.0141)

Abstract

The authors describe the use of platinum nanoclusters (PtNCs) as bimodal labels in a competitive immunoassay for immunoglobulin E (IgE). Both fluorometry and inductively coupled plasma – mass spectrometry (ICP-MS) are used. Optimization of the PtNCs synthesis process using lipoic acid as ligand was carried out. The time for synthesis and the effect of NaOH added to the PtNCs precursor mixture was optimized with the aim to obtain PtNCs with strong fluorescence and low size dispersity. Maximal fluorescence was obtained at excitation/emission wavelengths of 455/620 nm. The average diameter (1.5 nm) and crystal structure (face-centered cubic structure) of the PtNCs were determined by HR-TEM. It was calculated that each PtNC contains 116 Pt atoms at average. Labelling of the antibody (Ab) against IgE with PtNCs was optimized in terms of recognition capabilities and fluorescence signal. A molar ratio (Ab:PtNCs) of 1:11 is found to be best. A competitive immunoassay for IgE was developed and detection was carried out by using both ICP-MS (by measuring ^{195}Pt) and fluorometry. The limit of detection (LOD) of the fluoroimmunoassay is 0.6 ng mL^{-1} of IgE. The LOD of the ICP-MS method is as low as 0.08 ng mL^{-1}. The method was evaluated by analyzing four (spiked) serum samples by ICP-MS. No sample pretreatment excepting dilution is needed. Results compared favorably with those obtained by a commercial ELISA kit.

Keywords: fluoroimmunoassay; lipoic acid; one-pot synthesis; carbodiimide crosslinking; immunoprobe; elemental mass spectrometry.

Introduction

Elemental labels have shown a high potential for sensitive detection of biomolecules by inductively coupled plasma – mass spectrometry (ICP-MS) [1-3]. Within this context, single chelates [4], commercial polymers containing several lanthanide atoms covalently attached [5], metal nanoparticles (NPs) most commonly made of gold [6,7] with diameters in the order of 20-50 nm, and quantum dots (QDs) [8,9] have been successfully investigated as elemental labels. The use of labels with many atoms of a given metal per tag will allow high signal amplification, and thus, good sensitivity for detection of the corresponding biomolecule. Pure metal nanostructures, such as AuNPs, contain a core with atoms of just one metal. Thus they possess a higher number of detectable atoms per label unit volume [10] as compared to QDs (such as CdSe QDs) or to polymers containing lanthanides. Consequently, it is expected that pure metal nanostructures will provide greater signal amplification when comparing similar label sizes.

On the other hand, water soluble fluorescent metal nanoclusters (NCs) with sizes below 3 nm have shown a burgeoning interest for biomedical and biosensing applications [11,12]. The small volume of these NCs makes of interest their use for labelling of biomolecules such as antibodies (Ab), since they will have a lower risk of hindering the Ab recognition capabilities. Gold is, by far, the most common metal employed for the synthesis of fluorescent NCs [13]. Silver NCs [14,15] and copper NCs [16] are also frequently investigated. Nowadays, the synthesis of fluorescent NCs of other metals is pursued, such as iridium [17] and molybdenum [18].

Special efforts are being addressed towards the synthesis of platinum NCs (PtNCs). PtNCs show lower toxicity than QDs [19] and templates such as proteins, DNA, polymers and dendrimers have been investigated for the synthesis of water soluble PtNCs [20-24]. However, major drawbacks of big scaffolds are the difficulties both to remove the remaining free templates from the NCs in solution and to isolate the NCs from the big scaffold. In addition, when using polymers and dendrimers as templates it has been observed that reaction blanks often emit a noticeable fluorescence. In contrast, the synthesis of PtNCs using small thiolated ligands as stabilizing agents is an attractive alternative to easily isolate and purify fluorescent PtNCs [25,26]. Previous work in our laboratory has shown that the synthesis of fluorescent PtNCs using lipoic acid is feasible [26]; however, emission was low and studies about polydispersity were not undertaken.

Sensitive dual detection can be carried out with immunoprobes labelled with fluorescent NCs for biomolecules determination by fluorescence and elemental MS. Each of the detection methods will offer advantages and limitations. Therefore it is convenient to compare the analytical performance of both. Some works have been published about the bimodal detection concept using fluorescence and ICP-MS [8,27-29]. Bustos et al. [8] reported a comparison of both detection modes with CdSe/ZnS QDs through the measurement of Cd in the case of ICP-MS. Other examples include the use of a nanoprobe composed of europium chelated by 1,10-bis(50-chlorosulfo-thiophene-20-yl)-4,4,5,5,6,6,7,7-octafluorodecane-1,3,8,10-tetraone [28], the synthesis of hybrid labels containing both a DTPA chelate (coordinated with either ^{165}Ho or ^{111}In) and a Cy5 fluorescent dye [27], or by combining a fluorescent dye (Cy3) with upconversion NPs [29]. Those probes are compose either of just one metal atom or of atoms of different heteroatoms (e.g. CdSe), reducing the amplification capabilities by ICP-MS detection. Therefore, the described probes are not optimum when comparing expected signal amplification by ICP-MS and label size. Within this context, fluorescent NCs with small size and many atoms of a given metal are worth to be studied as labels for bimodal detection by fluorescence and ICP-MS.

In this work, the one pot synthesis of PtNCs with lipoic acid and sodium borohydride is optimized in terms of high fluorescence, low size dispersity and PtNCs stability. As a proof of concept, the synthesized PtNCs were bioconjugated, *via* carbodiimide, to anti-human IgE Ab (anti-h IgE) and evaluated for the determination of IgE in human serum by fluorescence and ICP-MS. We have selected this protein because IgE levels typically present in human serum are very low. Therefore, an analytical methodology with low limits of detection is required for its correct determination. To corroborate the IgE content obtained with the methodology using PtNCs labels, a commercial ELISA kit was employed for the same samples.

Experimental

Reagents and Materials

The synthesis of PtNCs was carried out using H_2PtCl_6 (8% wt; Sigma-Aldrich, USA; https://www.sigmaaldrich.com), lipoic acid (>98% powder; Across Organics, Belgium; http://www.acros.com) and $NaBH_4$ (98% powder, Sigma Aldrich). Labelling of the selected Ab with the PtNCs was carried out with 1-ethyl-3-(3-dimethylaminopropyl)

carbodiimide (EDC) (98% powder; Across Organics) and N-hydroxysuccinimide (NHS) (> 98% powder; Sigma-Aldrich). Amicon ultra centrifugal filter units (3 and 100 kDa pore size, Merck Millipore, Darmstadt, Germany; http://www.merckmillipore.com) were employed for purification.

ELISA microtitration plates (96 well; Thermo Fisher Scientific, Germany; https://www.thermofisher.com) were used to evaluate the recognition capabilities of the Ab labelled with PtNCs. A polyclonal anti-goat IgG labelled with horseradish peroxidase (whole molecule, produced in rabbit; Sigma-Aldrich) and a TMB substrate kit (Thermo Fisher Scientific) were employed in such studies.

The immunoassay for human-IgE determination was accomplished using an immunoprobe consisting of polyclonal anti-h IgE Ab (Ɛ-chain specific, produced in goat; Sigma Aldrich) labelled in our laboratory with the PtNCs. Native human IgE protein (Abcam, UK; https://www.abcam.com) was used as analytic standard. Bovine serum albumin (BSA) (99% powder, Merck, Germany) and phosphate buffered saline (PBS) (Sigma-Aldrich) solution with 0.05% of surfactant Tween 20 (Sigma-Aldrich) were employed in the immunoassay procedure. These immunoassays were carried out in two different mountings depending on the detection mode. Poly-L-lysine surface coated microscope slides (Electron Microscopy Sciences, Hatfield, PA, USA; http://www.electronmicroscopysciences.com) with an adhesive press-to-seal silicon isolator (Grace bio-labs, Oregon, USA; https://gracebio.com) were used for confocal microscopy in fluorescent detection, whereas the immunoassays were performed in ELISA microtitration plates (96 well; Thermo Fisher Scientific) when ICP-MS detection was performed.

Commercial human serum (from human male AB plasma, USA origin, sterile-filtered, Sigma-Aldrich) was used to investigate the applicability of the immunoassay with PtNCs. In addition, three clinical serum samples without any signs of relevant pathologies were supplied by the Instituto Oftalmológico Fernández-Vega (Spain). The study adheres to the tenets of the Declaration of Helsinki and full ethical approval was obtained for the Clinical Research Ethics Committee at the Asturias Central University Hospital (Spain). To validate the methodology, the IgE (human) ELISA Kit (Abnova, Taiwan; http://www.abnova.com) was used.

Other chemicals were aqua regia, prepared by mixing concentrated nitric acid (65%, Merck, Germany) and hydrochloric acid (37%, Fisher Scientific, USA) in a volume ratio of 1:3, used for PtNCs digestion prior to ICP-MS analysis, NaOH (97%, Merck) and

H_2SO_4 (Fisher Chemical, Thermo Fisher Scientific). Boric acid (99.5%, Sigma Aldrich) and KCl (99%, Sigma Aldrich) were employed to prepare the borate buffered saline (BBS). Deionized ultrapure water, resistivity 18.2 MΩ cm^{-1} (Purelab Flex 3&4, UK; https://www.elgalabwater.com), was used in all the experiments.

Instrumentation

Fluorescence measurements in solution were performed with a spectrofluorimeter (LS-50-B, Perkin Elmer, USA; https://www.perkinelmer.com). Also, a spectrophotometer (Cary 60 UV-VIS, Agilent Technologies, USA; https://www.agilent.com) was employed for absorption measurements of the synthesis precursors and PtNCs suspensions. A Suprasil quartz cuvette model 101-Qs from Hellma® (Sigma-Aldrich) was required for such purpose. A high-resolution transmission electron microscope (HR-TEM) (JEOL JEM-2100, Tokyo, Japan; https://www.jeol.co.jp) with an energy dispersive x-ray (EDX) spectrometer for microanalysis allowed morphological characterization of the PtNCs. Measurement of the Z-potential of PtNCs suspensions at different pHs was carried out with a Zetasizer Nano ZS (Malvern analytical Ltd, UK; https://www.malvernpanalytical.com).

A laser confocal microscope (DM IRE2; Leica, Germany, Germany; https://www.leica-microsystems.com) with a 63x oil immersion objective was employed for measurement of the immunoassays by fluorescence. Measurements with ICP-MS (Model 7500; Agilent Technologies) were taken for different purposes: to determine the platinum concentration in the PtNCs synthesis process, to confirm the platinum mass balance during the bioconjugation procedure, and to quantify the IgE protein in the competitive immunoassay measuring the platinum signal in each well of the ELISA plate.

An absorbance microplate reader (ELx800; Bio-Tek, USA; https://www.biotek.com), an ultrasonic bath (J.P. Selecta, Spain; http://grupo-selecta.com), a centrifuge (Gyrozen and Co., Rep of Korea; https://www.gyrozen.com/index.php), a magnetic stirring plate (Fisher Scientific), a vortex mixer (Labbox Labware, Spain; https://esp.labbox.com/) and a stove (Memmert, Spain, https://www.memmert.com) were other equipments used.

Fluorescence data processing was carried out using Image J software (National Institute of Health, Bethesda, USA; https://www.nih.gov) and immunoassay curves representation was done with the online data analysis tool MyAssays Ltd.

Synthesis of PtNCs and labelling of anti-h IgE

50 µmol (10.5 mg) of ligand (lipoic acid) was dissolved in 10 mL of deionized water in which 30 µL of freshly 2 M NaOH was previously added. The mixture was then homogenized with an ultrasonic bath until the ligand was completely dissolved. Then, 200 µL of 50 mM H_2PtCl_6 (1:5 molar final ratio of Pt:ligand) was added under stirring and 5 min later 400 µL of a 10 mM $NaBH_4$ solution was added dropwise (employing a syringe). After 15 h at room temperature under stirring, the excess of reagents were removed by ultrafiltration (3 kDa pore size Amicon): a first cycle at 1100 g for 10 min and then three washing steps with deionized H_2O at 1600 g for 10 min were carried out for such purpose. Once the volume was reduced, a small volume of yellow colored solution containing the PtNCs remained on the filter. Then, initial volume was restored. The purified solution was stored in the fridge.

100 µL of anti–h IgE Ab (100 µg mL^{-1}) was added in an Eppendorf tube followed by an excess of the PtNCs purified solution (198 µL, 1:20 molar ratio of Ab:PtNCs). As soon as the PtNCs solution was poured, vortex stirring was started. Then, 10 µL of a solution containing EDC and NHS were added with a molar ratio Ab:EDC:NHS of 1:1500:1500. After 2 h at room temperature with constant stirring, purification was performed by ultrafiltration (100 kDa pore size Amicon) with a first cycle at 1600 g for 10 min and three washing steps with deionized H_2O at 1600 g for 10 min. The purified solution was stored in the fridge.

Optimization of the immunoprobe composition

The ratio between the PtNCs label and the anti-h IgE in the immunoprobe was optimized through a spectrophotometric immunoassay, using a secondary Ab labelled with horseradish peroxidase. For such purpose, IgE was immobilized (100 µL/well of 5 µg mL^{-1} IgE) in an ELISA plate and incubated for 6 h at 37 °C. Then, the excess protein solution was removed and 200 µL/well of 1% BSA solution in 10 mM PBS (pH 7.4) was added to block the empty places in the well. The plate was incubated for 2 h at room temperature. Next, 100 µL/well of the anti-h IgE (1 µg mL^{-1}) was added and kept for 2 h at 37 °C. In this step, the Ab labelled with different molar ratios of PtNCs was employed for optimization purposes. After washing with 0.05% PBS-Tween 20, 100 µL/well of the anti-goat IgG peroxidase-labelled Ab (diluted 1:20000 in a buffer containing 1% PBS–BSA and 0.05% Tween 20) was added and incubated as above. Finally, the plate was

washed and treated with 100 µL/well of the TMB kit. The enzymatic reaction was stopped with 2 M sulfuric acid (100 µL/well) and detected in an absorbance plate reader (λ=450 nm).

Immunoassay with fluorescent detection using PtNCs as label

100 µL/well of IgE protein (10 µg mL^{-1}) containing EDC (1500:1 molar ratio of EDC:IgE) were added to wells on a poly-L-lysine coated microscope slide (EDC allowed to improve immobilization on the slides) and incubated during 2 h at 37 °C. Next, the IgE still in solution was removed and 200 µL/well of 1% BSA in 10 mM PBS (pH 7.4) was added to each well. The microscope slide was then incubated for 2 h at room temperature. Then, all wells were washed three times with 10 mM PBS (pH 7.4) and 0.05% Tween 20 (200 µL/well).

Concurrently, incubation of the immunoprobe containing PtNCs as label (100 µL of 10 µg mL^{-1}, expressed as Ab concentration) with 100 µL of the IgE standards or serum samples in an Eppendorf tube was carried out. To carry out the competitive reaction, this mixture was added to the previously treated wells (as described in the above paragraph) and incubated for 2 h at 37 °C. After the washing steps (three times) with PBS–Tween 20, the fluorescence was measured.

Immunoassay with ICP-MS detection using PtNCs as label

Despite the immunoassay steps were the same as those described in the above section, the mounting was changed because of the final step of the required protocol. An ELISA microwell plate was used for this purpose using ICP-MS detection. Once the last washing step was performed, 50 µL/well of a solution of 2 M H_2SO_4 was added in order to extract the PtNCs into the solution. After 10 min, the acid solutions were extracted from the wells to carry out the PtNCs digestion. 200 µL of aqua regia (HNO_3:3HCl)/tube were added to oxidize and dissolve platinum and then the tubes were introduced 20 min in an ultrasonic bath. Finally, a 1:200 dilution (5 mL final volume) of the samples was required to minimize the percentage of acid introduced into the ICP-MS (<3% v/v). ICP-MS measurements to determine the platinum concentration of PtNCs solutions were carried out by external calibration with pure platinum standards (concentrations from 0.05 ng g^{-1} to 20 ng g^{-1}) using iridium as internal standard (isotopes ^{195}Pt and ^{193}Ir were measured, respectively).

Human serum analysis

The applicability of the immunoassays with PtNCs was evaluated for the analysis of a commercial human serum and three clinical human serum samples (denoted as Serum 1, Serum 2 and Serum 3) using the same immunoassay procedure as for the IgE standards. Dilution of the sera was required to fit the concentrations of the samples into the linear range of the calibration plots. A 1:1000 dilution with PBS (pH 7.4) was carried out in the case of the commercial serum and the "Serum 1" clinical sample, whereas a 1:500 dilution was used for the rest of the sera.

The methodology with PtNCs as label was validated using a commercial ELISA kit.

Results and discussion

Synthesis of fluorescent PtNCs, their bioconjugation to a specific Ab and their subsequent application as label for detection of IgE is described. PtNCs have been chosen because they are fluorescent and also high amplification can be expected by ICP-MS detection (each label is composed of a cluster of platinum atoms). Therefore, they can be used for dual detection. $NaBH_4$ (as reducing agent) and lipoic acid (as small thiolated stabilizing agent) were used for the synthesis of PtNCs.

Synthesis of PtNCs using lipoic acid as ligand

PtNCs synthesized following the procedure described in the *Materials and Methods section* showed fluorescent emission with a maximum at 620 nm (see Fig. 1). The formation of the PtNCs was confirmed through absorbance measurements: as can be seen in Fig. S1 (*Electronic Supplementary Material*), the PtNCs suspension does not have the characteristic absorbance band of superficial plasmon resonance typical of bigger NPs. The blank of the synthesis was prepared under exactly the same steps than the PtNCs synthesis, excepting that the platinum salt was not added. As it is collected in Fig. 1, the emission signal for the reaction blank was negligible.

Lower $NaBH_4$ ratios decrease the reaction kinetics, giving rise to metal NCs of higher quality [14]. Therefore, in order to obtain PtNCs with higher fluorescence and less dispersity than those previously reported [26], the selected $NaBH_4$ molar ratio was lower than in the previous work (Pt:lipoic acid:$NaBH_4$ of 1:5:1 *versus* the 1:5:25 previously used). In addition, two experimental variables were evaluated in the optimization of the

PtNCs synthesis procedure: the synthesis duration and the effect of 2 M NaOH volume added to the PtNCs precursor mixture. Regarding the synthesis time, maximum signals were achieved after 13 h of synthesis at room temperature (Fig. S2 in *Electronic Supplementary Material*). This time period is longer than the 6 h previously recommended by Fernández et al. [26] and it can be justified in terms of the slower PtNCs synthesis kinetics due to the lower $NaBH_4$ molar ratio employed.

Regarding the effect of 2 M NaOH volume, Fig. 2 shows a comparison of fluorescence spectra for the purified PtNCs suspension obtained under synthesis with three different volumes of 2 M NaOH. Fluorescence signals were higher when using 30 μL as compared to 20 μL of 2 M NaOH. Furthermore, the concentration of platinum was measured by ICP-MS both in the filtered solutions collected during the purification process (i.e. the unreacted free platinum) and in the reconstituted suspensions (containing the PtNCs retained in the ultracentrifugation filter). The PtNCs synthesis yield was 60% when using 20 μL of 2 M NaOH, while the PtNCs synthesis yield was found to be 84% for the addition of 30 μL of 2 M NaOH to the reaction mixture. Here it should be noted that, as it is depicted in Fig. 2a, the increase of fluorescence is higher than the 24% synthesis yield difference, thus indicating that PtNCs of higher quality are synthesized with 30 μL of 2 M NaOH.

HR-TEM allowed to measure diameters of the synthesized PtNCs (Fig. 3a shows, as example, the PtNCs synthesized with 30 μL of 2 M NaOH). Average diameters were determined from individual PtNCs randomly observed in the HR-TEM photographs. A smaller size and lower dispersity (1.49 ± 0.025 nm for n=1800, 99% confidence interval, with the standard normal distribution) was found for the synthesis using 30 μL of 2 M NaOH as compared to 20 μL of 2 M NaOH (1.73 ± 0.044 nm for n=1800, 99% confidence interval, with the standard normal distribution). In addition, EDX measurements confirmed that platinum and sulphur were major elements of the synthesized PtNCs (the presence of sulphur is attributed to the lipoic acid used in the synthesis).

Concerning the NaOH volume employed in the synthesis, Fig. 2 also collects the fluorescence of the purified PtNCs synthesized with 50 μL of 2 M NaOH. Fluorescence signals were lower than in the case of 30 μL of 2 M NaOH and the PtNCs synthesis yield measured by ICP-MS was 73%. Considering that both fluorescence and synthesis yield were lower than for the synthesis with 30 μL of 2 M NaOH, no further studies under these experimental conditions were carried out.

From the above experiments, the addition of 30 μL of 2 M NaOH to the synthesis precursor mixture was selected. The PtNCs have a crystalline structure, face-centered cubic structure of platinum atoms, as observed by the selected area electron diffraction pattern (Fig. 3b). The knowledge of the crystal structure allowed to calculate the volume occupied by a unit cell ($6.04 \cdot 10^{-2}$ nm^3/cell), by considering the mass of a unit cell ($1.30 \cdot 10^{-21}$ g/cell) and the platinum density (21.45 g cm^{-3}). Additionally, dividing the average PtNC volume (diameter measured by HR-TEM and assuming spherical shape) by the unit cell volume it was calculated 29 crystal lattices *per* NC. As a face-centered cubic structure contains four platinum net atoms per unit cell, it can be determined that each PtNC is composed by 116 atoms of platinum on average. This figure is used to transform the platinum molar concentration determined by ICP-MS in the PtNCs purified suspension into PtNCs molar concentration. A value of $6.75 \cdot 10^{-6}$ mol PtNCs L^{-1} was experimentally obtained. In addition, the number of platinum atoms per NC is of interest to calculate the amplification expected in experiments with antibodies labelled with PtNCs and ICP-MS detection.

The effect of the pH was evaluated with the synthesized PtNCs. As can be observed in Fig. S3a (*Electronic Supplementary Material*), the fluorescence signal at 620 nm of the PtNCs suspension increased when lowering the pH from 12.4 up to 3.5. In addition, Z-potential measurements (Fig. S3b in the *Electronic Supplementary Material*) confirmed that PtNCs were stable at pHs higher than 3.5. Finally, stability experiments of PtNCs under different storage conditions and in different media were evaluated. Fig. S4a (*Electronic Supplementary Material)* shows high stability of the fluorescence signal (up to three months, which was the maximum period investigated) in ultrapure water and BBS medium. In the case of PBS, sensitivity starts to decrease after one day of storage. Fig. S4b (*Electronic Supplementary Material*) collects the time-drive of the PtNCs in ultrapure water during 2 h in the sample compartment of the fluorimeter (λ_{exc}=455 nm). No significant changes were observed in the fluorescence emission.

Selection of anti-h IgE:PtNC molar ratio in the bioconjugate

Different Ab:PtNC molar ratios (1:1, 1:10, 1:15, 1:20, 1:30 and 1:50) were assayed in the bioconjugation solution to label the anti-h IgE. To check if the Ab kept its functionality after being labelled with PtNCs, a study was made for the different ratios through a spectrophotometric immunoassay. For such purpose, IgE was immobilized in an ELISA plate and a secondary Ab labelled with horseradish peroxidase was employed

for detection. Fig. 4a depicts the absorbance at the different Ab:PtNCs molar ratios investigated. The recognition capabilities remained constant for 1:1, 1:10, 1:15 and 1:20 Ab:PtNC molar ratios (these values correspond to ratios added in the solution to label the Ab). However, the 1:30 ratio showed slight lower absorbance and the recognition capabilities were drastically lost for the Ab:PtNC molar ratio of 1:50. Therefore, in order to avoid the blocking of the recognition capabilities of the anti-h IgE due to the labelling process, Ab:PtNC molar ratios up to 1:20 were considered in the solutions to label the Ab.

Once the labelling of the Ab with PtNCs was achieved, the real number of PtNCs per Ab was calculated by measuring the platinum concentration (by ICP-MS) in labelled-Ab solutions containing a known amount of Ab. As it is collected in Table 1, labelling yields decreased with higher PtNCs ratios. For the 1:1 initial molar ratio in the labelling solution, not all Ab was labelled (77.6% labelling yield, thus corresponding to a real 1:0.77 Ab:PtNC molar ratio), while for the 1:20 initial ratio the labelling yield decreased up to 55.7%, corresponding to a real 1:11.13 Ab:PtNC molar ratio. Fig. 4b collects a comparison of the emission spectra of the bioconjugate containing 1:0.77 (1:1), 1:8.69 (1:15) and 1:11.13 (1:20) Ab:PtNC molar ratio and a PtNCs solution with the same dilution factor. It should be also highlighted that a linear regression was observed when plotting the different real bioconjugate molar ratios (up to 1:11.13 Ab:PtNC) *versus* measured signals, both for fluorescence at 620 nm and for platinum concentration determined by ICP-MS (data not shown).

Finally, platinum retained in the ELISA well plates (same experiment with data presented in Fig. 4a) was measured by ICP-MS. It is worth to highlight that a linear relationship was obtained by plotting the detected platinum mass (in ng) *versus* the real Ab:PtNCs molar ratio (Fig. S5 in *Electronic Supplementary Material*).

Immunoassays for IgE determination with fluorescence and ICP-MS detection

The determination of IgE using the immunoprobe containing PtNCs as label (with a Ab:PtNCs real molar ratio of 1:11.13) was carried out with a competitive immunoassay. Fig. 5a shows the inhibition curve by fluorescence detection following the optimized protocol detailed in the *Materials and Methods section* (i.e. immunoassay with fluorescent detection using PtNCs as label) for IgE standards. The calibration plot was fitted with a four-parameter equation with MyAssays Ltd. and different inhibitory concentration (IC) values were extracted from the graph. The limit of detection (LOD),

corresponding to IC_{10}, was 0.6 ng mL^{-1} of IgE, while the linear range (IC_{20}-IC_{80}) extended from 1.6 ng mL^{-1} up to 60 ng mL^{-1} of IgE. It is interesting to note that this LOD is slightly worse than the LOD previously reported using AuNCs as fluorescent labels (0.2 ng mL^{-1} of IgE) [30].

The inhibition curve by ICP-MS detection is collected in Fig. 5b. The calibration plot was fitted, as above, using a four-parameter equation. The LOD (IC_{10}) in this case is 0.08 ng mL^{-1} of IgE, which is lower than by fluorescent measurements with the same PtNCs immunoprobe. Such LOD is lower than the LOD of 0.2 ng mL^{-1} for IgE with fluorescent detection using an immunoprobe labelled with AuNCs [30]. Also, it compares favorably with most recently published methods for IgE determination in human serum (see Table 2) [30-38]. With ICP-MS detection of platinum, the linear range (IC_{20}-IC_{80}) extended from 0.10 ng mL^{-1} up to 2.6 ng mL^{-1} of IgE. In addition, it is interesting to note that for this linear interval we have observed that the plot of IgE molarity (x axis) used for calibration *versus* the detected platinum molarity (y axis) follows a linear trend, with a slope of 1264 units. This slope is in agreement with the signal amplification expected (the immunoprobe contains an average of 11.13 PtNCs per Ab and each NC is composed of 116 atoms of Pt on average).

Finally, considering the excellent LOD with ICP-MS, the immunoprobe labelled with PtNCs was investigated for the determination of IgE in human serum samples by ICP-MS. To evaluate the effect of the serum matrix, concentrations of $1 \cdot 10^{-4}$, $1.5 \cdot 10^{-4}$, $1.5 \cdot 10^{-3}$ and $2 \cdot 10^{-3}$ µg mL^{-1} of IgE were added to a commercial serum diluted 1:1000 and results were introduced (grey marks) into the inhibition curve (Fig. 5b). As can be observed, the spiked samples fit into the calibration plots, demonstrating that there are no matrix effects and it is possible to quantify IgE in diluted serum samples through calibration with PBS. Next, determination of IgE in four human serum samples was carried out with the immunoprobe labelled with PtNCs and results are collected in Table S1 (*Electronic Supplementary Material).* The applicability was proved through the successful comparison of the IgE concentrations with this methodology and those with a commercial kit (results are also collected in Table S1).

Conclusions

Synthesis of nearly monodisperse and high fluorescent PtNCs is not trivial, requiring a thorough optimization step. In this work, fluorescent PtNCs synthesized in

our laboratory were studied in terms of synthesis yield, size dispersity, platinum atoms per NC and PtNCs concentration. These PtNCs were used to label an anti-h IgE antibody as a proof of concept. Results showed that the immunoprobe selected as optimum contains an average of 11.13 PtNCs per Ab, which corresponds to about 1300 Pt atoms per Ab. Further studies to improve the size dispersity will be appropriate in order to use them in applications such as single-cell proteins detection.

The bimodal detection capabilities (fluorescence and ICP-MS) of PtNCs were investigated and compared through a competitive immunoassay for sensitive detection of IgE. The huge amplification with ICP-MS detection gave rise to a better LOD as compared to the fluoroimmunoassay. In any case, it should be kept in mind that fluorescence measurements are cheaper than those performed by ICP-MS. Therefore, the fluoroimmunoassay can be selected when sensitivity requirements allow it. In contrast, the low LOD by ICP-MS points out to the use of this detection system for those analyses requiring high sensitivity or for small sample volumes. In addition, it should be noted that in our experiments we have detected ^{195}Pt which has a 33.775% isotopic abundance. Therefore, the LOD by ICP-MS should be improved with isotopically-enriched PtNCs.

Finally, it is worth to highlight that the combination of the PtNCs immunoprobe with ICP-MS detection opens the door to multiplexed protein analysis by using isotopically-enriched NCs. In the particular case of platinum, it is possible to obtain six different immunoprobes (^{190}Pt, ^{192}Pt, ^{194}Pt, ^{195}Pt, ^{196}Pt, and ^{198}Pt) with the same synthesis protocol, thus increasing both the multiplexing capabilities and the sensitivity of the analysis. In addition, future research related to bioimaging studies by laser ablation coupled to ICP-MS using PtNCs labels should be expected.

Conflict of interest

There are no conflicts to declare.

Acknowledgements

This work was financially supported through project CTQ2016-79015-R by Agencia Estatal de Investigación (Spain) and FEDER. A. Lores-Padín and B. Fernández respectively acknowledge the FPU Grant (Ref. MECD-17-FPU16/01363; Ministry of Education) and the contract RYC-2014-14985 through the "Ramón y Cajal Program" (Ministry of Economy and Competitiveness).

References

[1] Baranov VI, Quinn Z, Bandura DR, Tanner SD (2002) A sensitive and quantitative element-tagged immunoassay with ICPMS detection. Anal Chem 74:1629–1636.

[2] Liu Z, Li X, Xiao G, Chen B, He M, Hu B (2017) Application of inductively coupled plasma mass spectrometry in the quantitative analysis of biomolecules with exogenous tags: A review. Trends Anal. Chem 93:78–101.

[3] Zhang C, Wu F, Zhang Y, Wang X, Zhang X (2001) A novel combination of immunoreaction and ICP-MS as a hyphenated technique for the determination of thyroid-stimulating hormone (TSH) in human serum. J Anal At Spectrom 1:1393–1396.

[4] Mairinger T, Wozniak-Knopp G, Rüker F, Koellenspergerd G, Hann S (2016) Element labeling of antibody fragments for ICP-MS based immunoassays. J Anal At Spectrom 31:2330–2337.

[5] Perez E, Bierla K, Grindlay G, Szpunar J, Mora J, Lobinski R (2018) Lanthanide polymer labels for multiplexed determination of biomarkers in human serum samples by means of size exclusion chromatography-inductively coupled plasma mass spectrometry. Anal Chim Acta 1018:7–15.

[6] He Y, Chen D, Li M, Fang L, Yang W, Xu L, Fu F (2014) Rolling circle amplification combined with gold nanoparticles-tag for ultrasensitive and specific quantification of DNA by inductively coupled plasma mass spectrometry. Biosens Bioelectron 58:209–213.

[7] Xiao G, Chen B, He M, Shi K, Zhang X, Li X, Wu Q, Pang D, Hu B (2017) Determination of avian influenza A (H9N2) virions by inductively coupled plasma mass spectrometry based magnetic immunoassay with gold nanoparticles labeling. Spectrochim Acta Part B 138:90–96.

[8] Bustos ARM, Trapiella-Alfonso L, Encinar JR, Costa-Fernández JM, Pereiro R, Sanz-Medel A (2012) Elemental and molecular detection for quantum dots based immunoassays: A critical appraisal. Biosens Bioelectron 33**:**165–171.

[9] García-Cortes M, Encinar JR, Costa-Fernández JM, Sanz-Medel A (2016) Highly sensitive nanoparticle – based immunoassays with elemental detection: Application to prostate-specific antigen quantification. Biosens Bioelectron 85:128–134.

[10] Tvrdonova M, Vlcnovska M, Pompeiano L, Viktor V, Vojtech K, Lena AA, Jakubowski N, Vaculovicova M, Vaculovic T (2019) Gold nanoparticles as labels for immunochemical analysis using laser ablation inductively coupled plasma mass spectrometry. Anal Bioanal Chem 411:559–564.

[11] Song X-R, Goswami N, Yang H-H, Xie J (2016) Functionalization of metal nanoclusters for biomedical applications. Analyst 141:3126–3140.

[12] Zhang L, Wang E (2014) Metal nanoclusters: New fluorescent probes for sensors and bioimaging. Nano Today 9:132–157.

[13] Zhang Y, Zhang C, Xu C, Wang X, Liu C, Waterhouse GIN, Wang Y, Yin H, Ultrasmall Au nanoclusters for biomedical and biosensing applications: a mini-review. Talanta 200:432–442.

[14] Zheng K, Yuan X, Goswami N, Zhang Q, Xie J (2014) Recent advances in the synthesis, characterization, and biomedical applications of ultrasmall thiolated silver nanoclusters. RSC Adv 4**:**60581–60596.

[15] Valencia E, Cruz-Alonso M, Álvarez L, González-Iglesias H, Fernández B, Pereiro R (2019) Fluorescent silver nanoclusters as antibody label in a competitive immunoassay for the complement factor H. Microchim. Acta 186:429 https://doi.org/10.1007/s00604-019-3554-y.

[16] Hu X, Lui T, Zhuang Y, Wang W, Li Y, Fan W, Huang Y (2016) Recent advances in the analytical applications of copper nanoclusters. Trends Anal Chem **77**:66–75.

[17] Cui M, Wang C, Yang D, Song Q (2018) Fluorescent iridium nanoclusters for selective determination of chromium(VI). Microchim Acta 185:8 https://doi.org/10.1007/s00604-017-2553-0.

[18] Sharma AK, Pandey S, Sharma N, Wu H-F (2019) Synthesis of fluorescent molybdenum nanoclusters at ambient temperature and their application in biological imaging. Mater Sci Eng C 99:1–11.

[19] Huang X, Ishitobi H, Inouye Y (2016) Formation of fluorescent platinum nanoclusters using hyper-branched polyethylenimine and their conjugation to antibodies for bio-imaging. RSC Adv 6:9709–9716.

[20] Li J, Zhu J-J, Xu K (2014) Fluorescent metal nanoclusters: From synthesis to applications. Trends Anal Chem 58:90–98.

[21] Tanaka S, Miyazaki J, Tiwari DK, Jin T, Inouye Y (2011) Fluorescent platinum nanoclusters: synthesis, purification, characterization, and application to bioimaging, Angew Chem Int Ed 50:431–435.

[22] Xu N, Li H-W, Yue Y, Wu Y (2016) Synthesis of bovine serum albumin protected high fluorescence Pt16- nanoclusters and their application to detect sulfide ions in solutions. Nanotechnology 27**:**425602 (7 pp).

[23] Xu N, Li H-W, Wu Y (2017) Hydrothermal synthesis of polyethylenimine-protected high luminescent Pt-nanoclusters and their application to the detection of nitroimidazoles. Anal Chim Acta 958:51–58.

[24] Yu C-J, Chen T-H, Jiang J-Y, Tseng W-L (2014) Lysozyme-directed synthesis of platinum nanoclusters as a mimic oxidase. Nanoscale 6:9618–9624.

[25] Chen D, Gao S, Ge W, Li Q, Jiang H, Wang X (2014) One-step rapid synthesis of fluorescent platinum nanoclusters for cellular imaging and photothermal treatment. RSC Adv 4:40141–40145.

[26] Fernández JG, Trapiella-Alfonso L, Costa-Fernández JM, Pereiro R, Sanz-Medel A (2015) Aqueous synthesis of near-infrared highly fluorescent platinum nanoclusters. Nanotechnology 26:215601 (7 pp).

[27] Buckle T, van der Wal S, van Malderen SJM, Müller L, Kuil J, van Unen V, Peters RJB, van Bemmel MEM, McDonnell LA, Velders AH, Koning F, Vanhaeke F, van Leeuwen FWB (2017) Hybrid imaging labels: providing the link between mass spectrometry-based molecular pathology and theranostics. Theranostics 7:624–633.

[28] Feng D, Tian F, Qin W, Qian X (2016) A dual-functional lanthanide nanoprobe for both living cell imaging and ICP-MS quantification of active protease. Chem Sci 7: 2246–2250.

[29] Yang B, Zhang Y, Chen B, He M, Yin X, Wang H, Li X, Hu B (2017) A multifunctional probe for ICP-MS determination and multimodal imaging of cancer cells. Biosens Bioelectron 96:77–83.

[30] Cruz-Alonso M, Trapiella-Alfonso L, Costa-Fernández JM, Pereiro R, Sanz-Medel A (2016) Functionalized gold nanoclusters as fluorescent labels for immunoassays: Application to human serum immunoglobulin E determination. Biosens Bioelectron 77:1055–1061.

[31] Hahn YK, Jin Z, Kang JH, Oh E, Han MK, Kim HS, Jang JT, Lee JH, Cheon J, Kim SH, Park HS, Park JK (2007) Magnetophoretic immunoassay of allergen-specific IgE in an enhanced magnetic field gradient. Anal Chem 79:2214–2220.

[32] Chen HX, Busnel JM, Peltre G, Zhang XX, Girault HH (2008) Magnetic beads based immunoaffinity capillary electrophoresis of total serum IgE with laser-induced fluorescence detection. Anal Chem 80:9583–9588.

[33] Peng Q, Cao Z, Lau C, Kai M, Lu J (2011) Aptamer-barcode based immunoassay for the instantaneous derivatization chemiluminescence detection of IgE coupled to magnetic beads. Analyst 136:140–147.

[34] Cheow LF, Han J (2011) Continuous signal enhancement for sensitive aptamer affinity probe electrophoresis assay using electrokinetic concentration. Anal Chem 83:7086–7093.

[35] Chinnasamy T, Segerink LI, Nystrand M, Gantelius J, Andersson H (2014) A lateral flow paper microarray for rapid allergy point of care diagnostics. Analyst 139: 2348–2354.

[36] Cao J, Wang H, Liu Y (2015) Petal-like CdS nanospheres-based electrochemiluminescence aptasensor for detection of IgE with gold nanoparticles amplification. Spectrochim Acta A 151:274–279.

[37] Li Z, Li Z, Niu Q, Li H, Vuki M, Xu D (2017) Visual microarray detection for human IgE based on silver nanoparticles. Sensor Actuat B-Chem 239:45–51.

[38] Yescas-González T, Leonard A, Gaude V, Delplanque A, Barre A, Rougé P, Garnier L, Bienvenu F, Bienvenu J, Zelsmanna M, Picard E, Peyrad D (2019) IgE detection in allergic patient's serum by absorption analysis of biofunctionalised microparticles. Microelectron Eng 207:27–32.

Table 1. Labelling yield of the Ab in the bioconjugation process determined by ICP-MS.

Ab:PtNC molar ratio in the solution for Ab labelling	**1:1**	**1:10**	**1:15**	**1:20**
Labelling yield, % (ICP-MS measurements)	77.60%	62.41%	57.92%	55.67%
Measured ("real") Ab:PtNC molar ratio in the labelled Ab	1:0.77	1:6.24	1:8.69	1:11.13

Table 2. Overview of recently reported nanomaterial and/or based optical sensitive methods for determination of Ig E.

	Materials used	Method	LOD ($ng\ mL^{-1}$)	Ref.
Commercial kits	-	Classical ELISA absorbance (ABNOVA).	12	-
	-	Microarray chip ImmunoCAP ISAC (Thermo Fisher)	0.24	-
Published methods	Superparamagnetic Fe_3O_4 NPs	Magnetophoretic immunoassay	0.1	[31]
	Tosyl-activated superparamagnetic beads	Immunoaffinity capillary electrophoresis. Fluorescence detection	2.4	[32]
	Chemiluminescence reagent acts as the signaling molecule and polystyrene beads as the amplification platform	Aptamer-barcode enhanced chemiluminescence immunosensor	0.87	[33]
	Poly(dimethylsiloxane) microfluidic electrokinetic concentration chip	Aptamer affinity probe capillary electrophoresis. Fluorescence detection	7	[34]
	Bioconjugated AuNPs	Lateral flow microarrays	2.4	[35]
	CdS nanospheres and AuNPs	Electrochemiluminescence aptasensor	0.02	[36]
	Aptamer modified with AgNPs	Visual microarray	20	[37]
	Polystyrene and super-paramagnetic particle complexes	Microparticle-based competitive immunoassay and visible light absorption	24	[38]
	AuNCs	Competitive fluoroimmunoassay	0.20	[30]
	PtNCs	Competitive immunoassay (fluorescence and ICP-MS)	0.60 (fluorescence) & 0.08 (ICP-MS)	This work

Legends of figures

Figure 1. PtNCs fluorescence characterization. Excitation (gray line) and emission (black line) spectra of PtNCs in ultrapure water (λ_{exc}=455 nm, λ_{em}=620 nm). The dotted black line corresponds to the emission spectrum of the synthesis blank. The plot depicts normalized intensities, given 100 value to the maximum fluorescence signal observed at 620 nm.

Figure 2. Effect of 2 M NaOH volume added to the synthesis mixture of precursors on PtNCs fluorescence. Continuous black color: 30 μL NaOH, continuous gray color: 50 μL NaOH, dotted gray color: 20 μL NaOH. For comparison purposes the fluorescence was measured at the same pH for the three syntheses.

Figure 3. Structural characterization of PtNCs. (a) HR-TEM image of the PtNCs synthesized under the optimum experimental conditions, and (b) Selected area electron diffraction pattern of a PtNC determined by HR-TEM where the four inner electron diffraction rings from the NC are distinguished. The rings diameter in nm^{-1} units are collected at the top right of the image. The radius of the rings diffraction ($d_{spacing}$) confirms the crystal structure of the PtNCs to be compared with the Pt metal $d_{spacing}$ collected in bibliography.

Figure 4. PtNCs bioconjugation optimization. (a) Absorbance measured in ELISA well plates for different Ab:PtNC molar ratios employed in the reaction solution for Ab labelling. Uncertainties represent the standard deviations of the mean of three independent measurements, and (b) Comparison of emission spectra for PtNCs (dotted gray line) and Ab labelled with PtNCs using different Ab:PtNC molar ratios, 1:20 (black line), 1:15 (tinny dotted line) and 1:1 (dotted black line), in the bioconjugation process (same pH and same PtNCs dilution in the spectra).

Figure 5. Calibration curves for IgE determination by competitive format, using the IgE immunoprobe containing the molar ratio 1:11.13 Ab:PtNCs. (a) Calibration plot by fluorescence detection with laser confocal microscopy (λ_{ex}=470 nm, range λ_{em}=610-650 nm). The y-axis corresponds to the normalized integrated density signal fluorescence from the PtNCs in each well (integrated by ImageJ program). Uncertainties represent the standard deviations of the mean of three independent measurements. (b) Calibration plot by ICP-MS (^{195}Pt ion signal intensity was measured). The y-axis corresponds to the concentration of Pt, calculated by an external calibration curve with internal standard (^{193}Ir). The black marks belong to the IgE protein standards in PBS solution for building the calibration curve and the circle marks correspond to the enriched sera (with different concentrations of IgE standard). Uncertainties represent the standard deviations of the mean of three independent measurements."

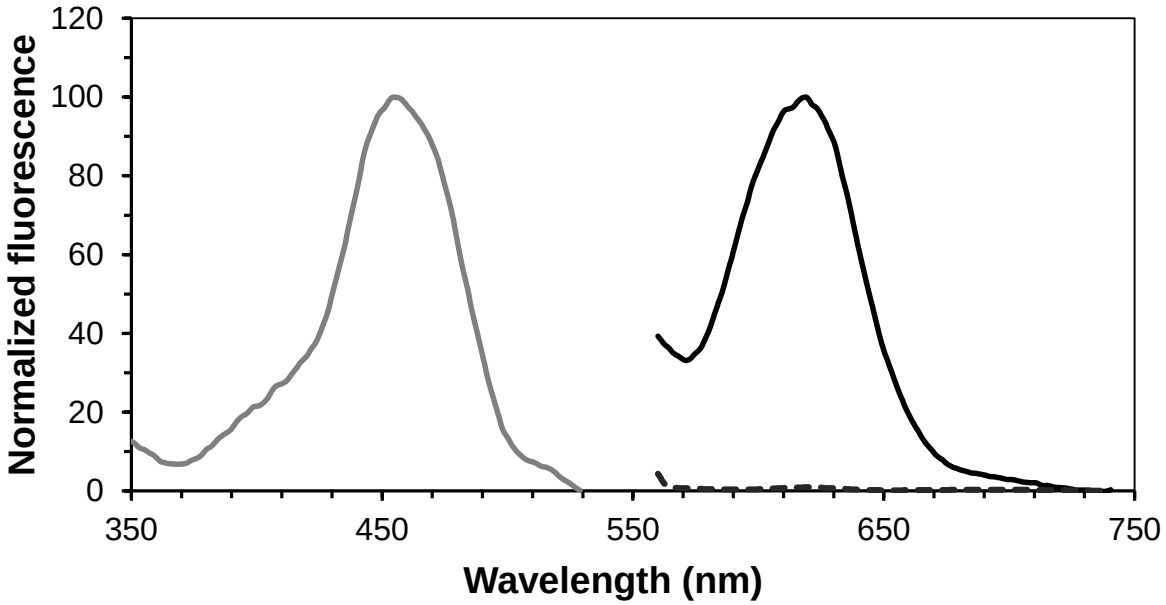
Normalized fluorescence
120
100
80
60
40
20
0
350
450
550
650
750
Wavelength (nm)

Figure 1

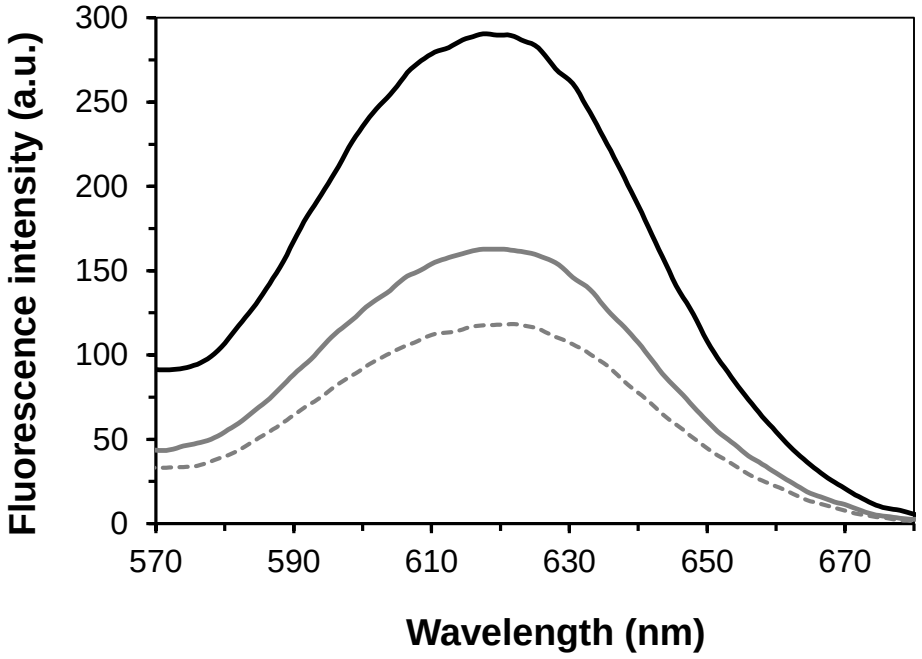
Fluorescence intensity (a.u.)
300
250
200
150
100
50
0
570
590
610
630
650
670
Wavelength (nm)

Figure 2

(a)

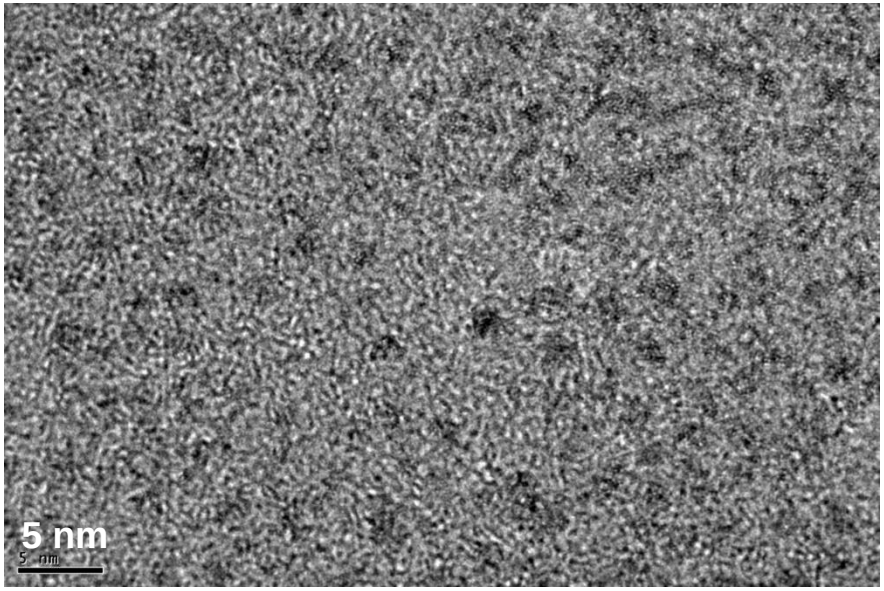

(b)

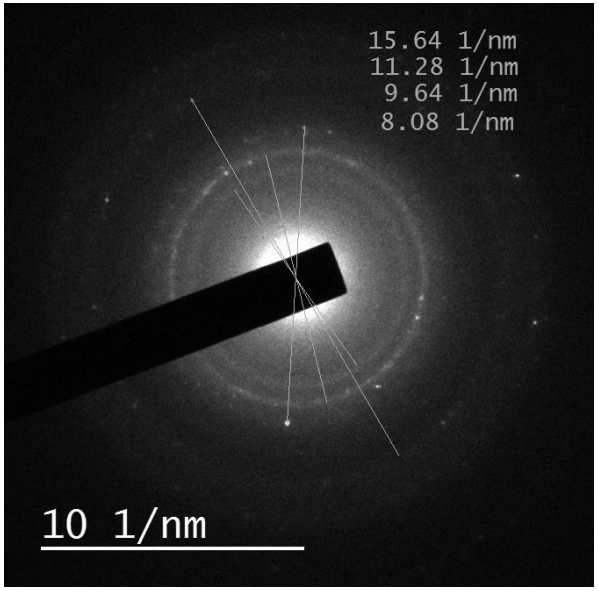

Figure 3

(a)

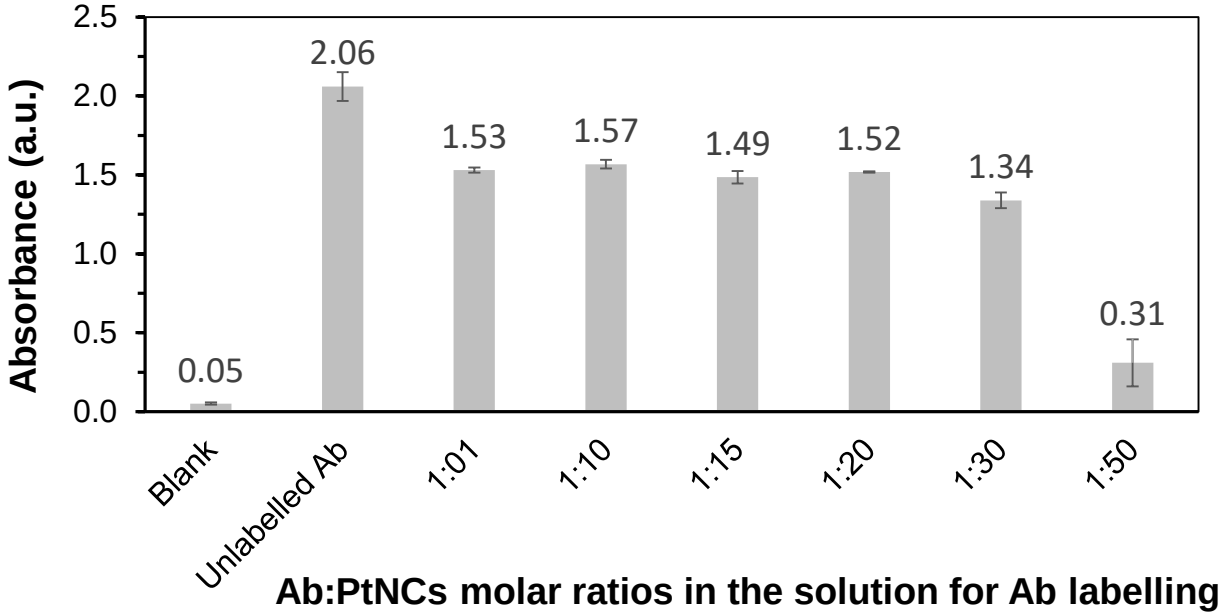
Absorbance (a.u.)
2.5
2.0
1.5
1.0
0.5
0.0
2.06
1.53
1.57
1.49
1.52
1.34
0.31
0.05
Blank
Unlabelled Ab
1:01
1:10
1:15
1:20
1:30
1:50
Ab:PtNCs molar ratios in the solution for Ab labelling

(b)

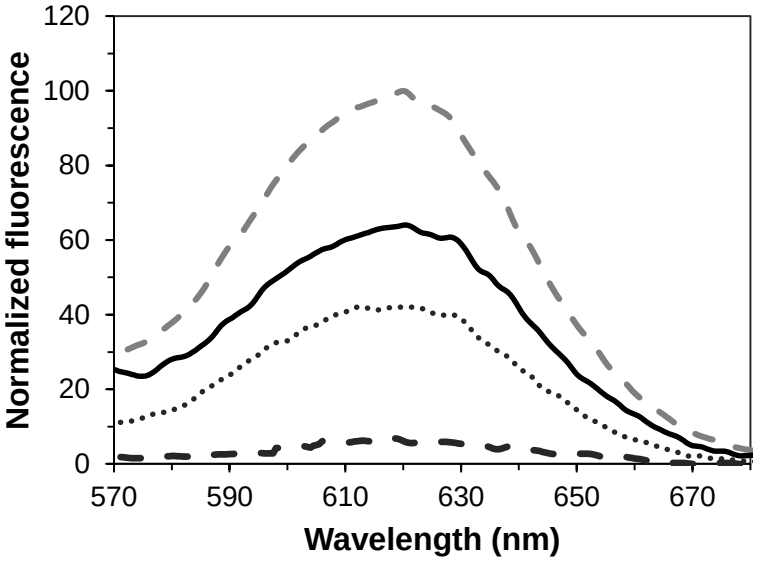
Normalized fluorescence
120
100
80
60
40
20
0
570
590
610
630
650
670
Wavelength (nm)

Figure 4

(a)

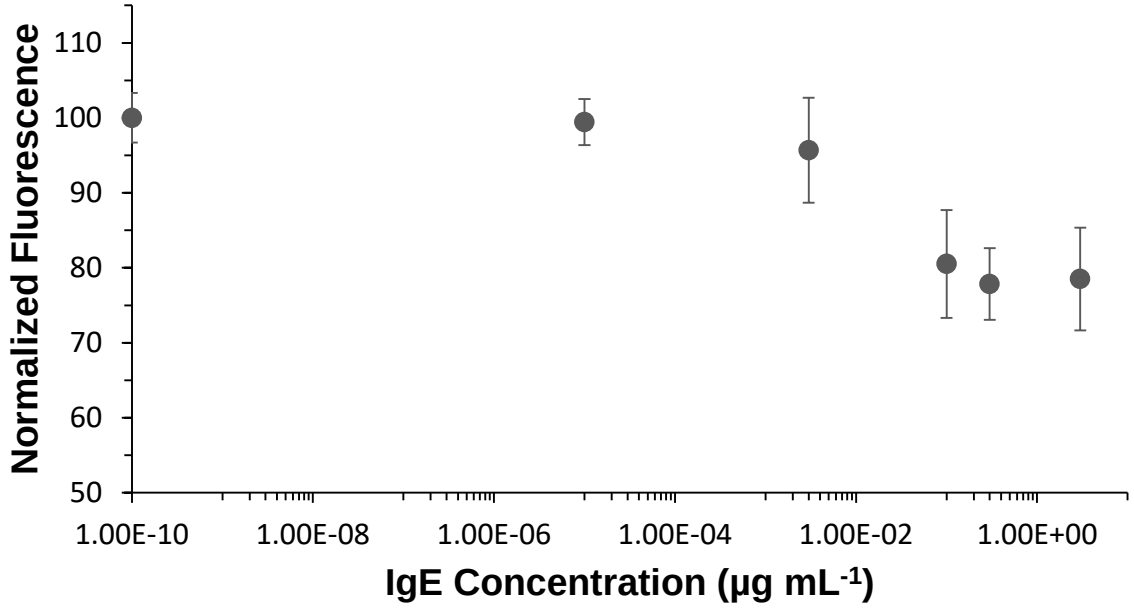
Normalized Fluorescence
110
100
90
80
70
60
50
1.00E-10
1.00E-08
1.00E-06
1.00E-04
1.00E-02
1.00E+00
IgE Concentration (µg mL-1)

(b)

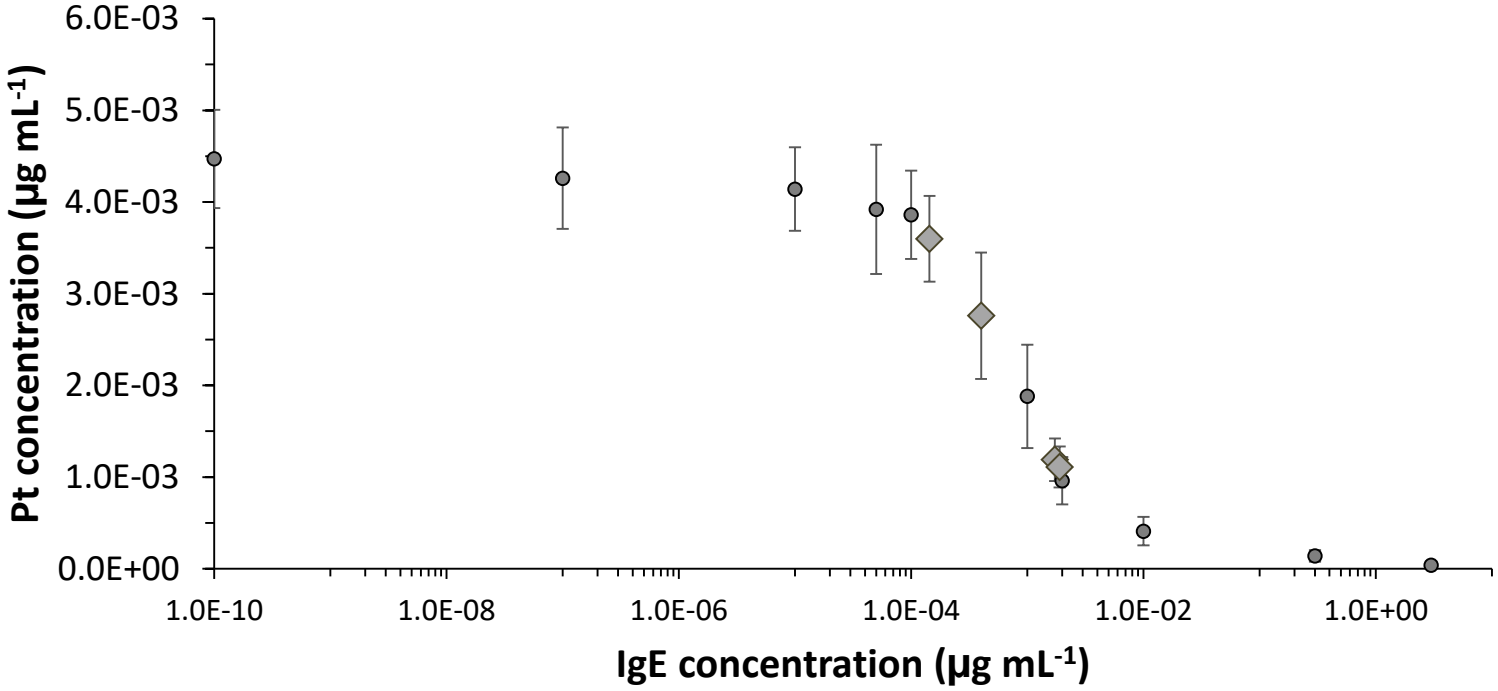
Pt concentration (µg mL-1)
6.0E-03
5.0E-03
4.0E-03
3.0E-03
2.0E-03
1.0E-03
0.0E+00
1.0E-10
1.0E-08
1.0E-06
1.0E-04
1.0E-02
1.0E+00
IgE concentration (µg mL-1)

Figure 5